

## The thermal, optical, flame retardant, and morphological consequence of embedding diacid-capped ZnO into the recycled PET matrix

Shadpour Mallakpour,<sup>1,2,3</sup> Mashal Javadpour<sup>1</sup>

<sup>1</sup>Organic Polymer Chemistry Research Laboratory, Department of Chemistry, Isfahan University of Technology, Isfahan 84156-83111, I. R. Iran

<sup>2</sup>Nanotechnology and Advanced Materials Institute, Isfahan University of Technology, Isfahan 84156-83111, I. R. Iran

<sup>3</sup>Department of Chemistry, Center of Excellence in Sensors and Green Chemistry, Isfahan University of Technology, Isfahan 84156-83111, I. R. Iran

Correspondence to: S. Mallakpour (E-mail: mallakpour84@alumni.ufl.edu)

**ABSTRACT:** We extended our work to a fast and facile nanocomposites (NCs) manufacturing by incorporation of ZnO nanoparticles (NPs) on to a recycled poly(ethylene terephthalate) PET as a polymer matrix prepared by a dissolution/precipitation method. The surface of ZnO NPs was functionalized with synthesized optically active diacid containing alanine amino acid. Organo-modified NPs which provided using solution blending technique through ultrasonic irradiation, were embedded into recycled PET. PET@ZnO/DA NCs containing different loadings of functionalized NPs (1, 3, 5 wt %) were investigated by thermal gravimetric analysis, field emission scanning electron microscopy, transmission electron microscopy, X-ray diffraction, Fourier transform infrared spectroscopy and UV–visible spectroscopy. Morphological studies revealed uniformly dispersed ZnO/DA NPs in the polymer matrix. The crystalline nature of PET slightly improved as a function of the NPs concentration. Char yield in TGA and LOI values indicated that the obtained NCs were capable of exhibiting flame retardant properties. The NCs were found to exhibit more absorbance in the UV and visible region in compare to the neat PET. The effect of ultrasonication in different solvent on the morphology of the recycled polymer particle was also studied. © 2016 Wiley Periodicals, Inc. *J. Appl. Polym. Sci.* **2016**, *133*, 43433.

**KEYWORDS:** composites; nanoparticles; poly(ethylene terephthalate); recycling; thermogravimetric analysis; X-ray

Received 26 September 2015; accepted 7 January 2016

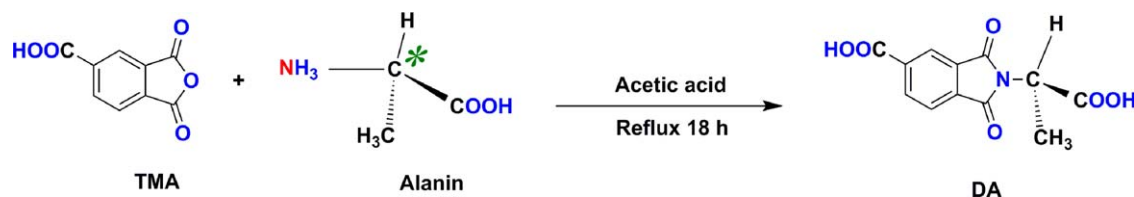
DOI: 10.1002/app.43433

### INTRODUCTION

Recycling is the procedure of collecting and processing materials to prevent waste of potentially useful and reduce the consumption of fresh raw materials. Recycling in different way can help human, community, and the environment by saving money, energy, and natural resources.<sup>1,2</sup> Biological recycling refers to biodegradation of plastics by microorganisms and enzymes.<sup>3</sup> Mechanical recycling discusses operations that aim to recover plastics waste via mechanical processes without significant changes in the chemical structures. Thermal recycling is the process to generate electricity and provide heat from incinerating plastic. Chemical recycling refers to operations that aim to chemically degrade the collected plastics waste into its monomers or other basic chemicals.<sup>4–7</sup> By dissolution/precipitation recycling process it is possible to reuse the waste PET by dissolving the waste PET in an appropriate solvent and then reprecipitation of PET using nonsolvent thorough washing of the material obtained, and drying.<sup>8,9</sup>

PET is a kind of low cost engineering plastic that is in common usage in many products nowadays and is easy recyclable. Because it is lightweight, economical, and shatter proof, PET plastic offered unique marketing and lifestyle benefits. PET is the most widely recycled plastic in the world that is used for many end products including packaging for detergents, cosmetics, carpets, foils, car parts, or back into PET bottles.<sup>7,10,11</sup> Recycled PET has lower price than the corresponding virgin polymer price because of the assumption that the quality of recycle one is lower than that of virgin materials. Then this suggests that addition of nano-sized metal oxide fillers to recycled PET may be beneficial as an adjunct to the efficiency of polymer.

Polymer nanocomposite (NC) is a two-phase system, that one dimension of the reinforcing filler is on the nanometer scale (0–100 nm). Depending on the type, size, also dispersion and nanoparticles (NP)s surface, the interfaces determine the novel properties of NCs.<sup>12</sup> NPs are a varied form of basic elements



**Scheme 1.** Synthesis of DA. [Color figure can be viewed in the online issue, which is available at [wileyonlinelibrary.com](http://wileyonlinelibrary.com).]

derived by altering their atomic and molecular properties of elements.<sup>13</sup> Biosafe ZnO NPs, as a common industrial additive,<sup>14</sup> are available in different forms and structures and their properties remain stable in the atmosphere. These transition metal oxides exhibit antibacterial, antifungal and UV filtering properties.<sup>15–17</sup> ZnO NPs incorporation into most material processes can achieve due to their specific compatibility towards both aqueous and organic solvents.<sup>18</sup> Furthermore, it has catalytic activity especially in nano form that enhances their vacancies due to its large surface area and the presence of uncoordinated atoms at corners and edges.<sup>19</sup> In spite of these advantages, NPs do have limitations; for instance, their small size and large surface area can lead to particle–particle agglomeration, making physical management of NPs difficult in liquid and dry forms. These practical difficulties have to be overcome before NPs can be applied as modifier in NC manufacturing.<sup>20</sup> Binding of organic coupling agents onto the surface of NPs, acts as a bridge between NPs and organic matrix. Currently, various coupling agents such as H550,<sup>21</sup> citric acid,<sup>22</sup> and stearic acid<sup>23</sup> have been examined on the surface of ZnO NPs and compared to the NC filled with unmodified ZnO<sup>23</sup>; results showed significant improvement in the NCs properties. In other earlier reports, the effect of incorporation of DAs based on amino acids into the different types of polymeric structure was examined and results displayed that the synthetic materials from these DAs were biocompatible, biodegradable, and nontoxic.<sup>24,25</sup> So from biological point of view, it can be concluded that bioactive DAs are the suitable selection for the modification of safe ZnO NPs.

This approach involves PET recycling in dissolution/precipitation method and functionalization of ZnO NPs with optically active and biocompatible dicarboxylic acid (DA) containing natural alanine amino acid to improve their dispersion and compatibility in polymer matrix.<sup>25</sup> Then a facile and simple approach for the manufacturing of novel PET@ZnO/DA NCs is described. The surface modification of ZnO and effects of modified NPs on the properties of the obtained NCs were investigated and characterized by Fourier transform infrared spectroscopy (FT-IR), thermogravimetric analysis (TGA) and

X-ray diffraction (XRD) and UV–vis spectroscopy. The surface morphology of PET@ZnO/DA NCs was characterized by field emission scanning electron microscopy (FE-SEM) and transmission electron microscopy (TEM).

## EXPERIMENTAL

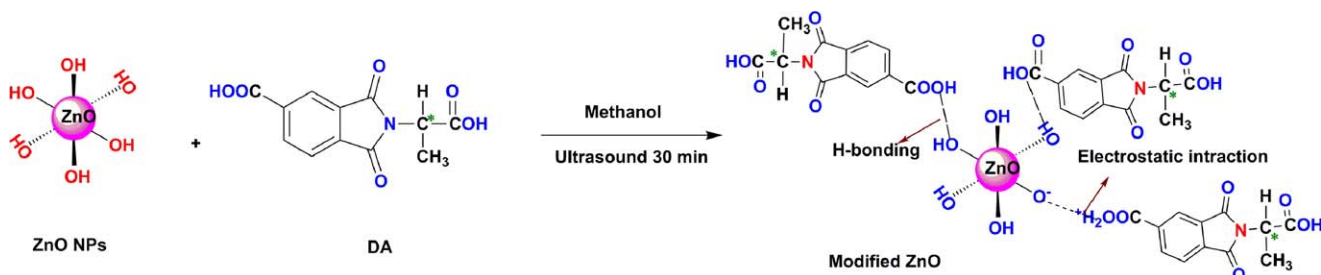
### Materials

The PET used for the preparation of the NCs in all experiments, was obtained from PET beverage bottles by recycling. Trimellitic anhydride (TMA, C<sub>9</sub>H<sub>4</sub>O<sub>5</sub>, *M<sub>w</sub>*: 192.01 g/mol), L-alanine amino acid (C<sub>3</sub>H<sub>7</sub>NO<sub>2</sub>, *M<sub>w</sub>*: 89.09 g/mol), methanol, ethanol, hydrochloric acid, dimethyl sulfoxide (DMSO), dimethylacetamide (DMAc), as well as glacial acetic acid were purchased from Merck Chemical Co. and were used without further purification. Nano-sized ZnO powder with average particle size of <25 nm and specific surface area >80 m<sup>2</sup> g<sup>-1</sup> was purchased from Neutrino Co. NPs were dried at 400 °C for 4 h before surface modification.

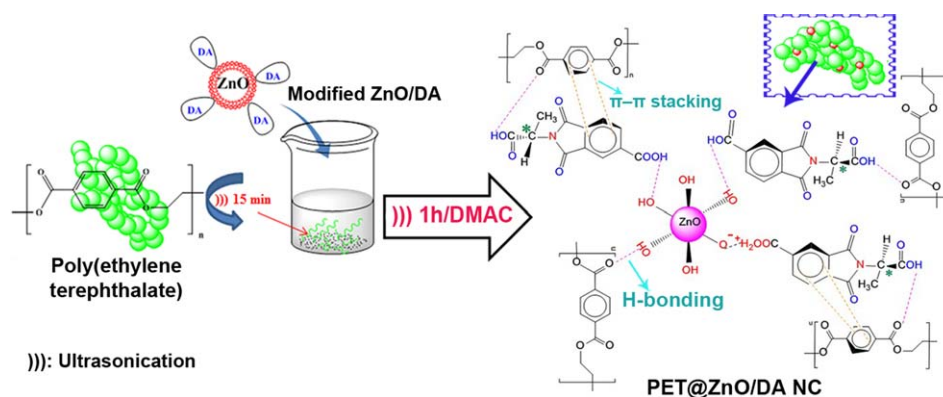
### Procedure

**Surface Modification of ZnO NPs with DA.** Optically active DA containing L-alanine amino acid was prepared under ultrasonic irradiation conditions which were reported before (Scheme 1). Surface modification of ZnO NPs was carried out with DA under ultrasonic irradiation conditions.<sup>25</sup> Firstly; 0.015 g of DA (15 wt % with respect to the ZnO) was added to the mixture of 0.10 g of ZnO NPs that was suspended in absolute methanol. The combination was stirred at room temperature for 24 h and ultrasonicated for 30 min to obtain ZnO/DA (Scheme 2). The modified ZnO/DA NPs were dried at room temperature. Scheme 2 has illustrated different interactions between the different functional groups of the DA and –OH on the surface of ZnO NPs.

**PET Recycling.** Before charging PET in the reactor, the bottles were cut down into 1 mm × 1 mm to 6 mm × 6 mm flakes and washed by hot water. DMSO was solvent in the recycling process and the mixture of 1 g of PET flakes with 20 mL DMSO was shaking vigorously at atmospheric pressure under heating to dissolve PET flakes into the solvent. The vapor products can be recycled in



**Scheme 2.** Modification of ZnO NPs with DA. [Color figure can be viewed in the online issue, which is available at [wileyonlinelibrary.com](http://wileyonlinelibrary.com).]



**Scheme 3.** Fabrication of PET@ZnO/DA NCs. [Color figure can be viewed in the online issue, which is available at [wileyonlinelibrary.com](http://wileyonlinelibrary.com).]

a cold trap (using a cold water condenser) to liquid products. After dissolution of the waste PET in DMSO, the cold water was added instantly that resulted in complete precipitation of PET. The polymer grains were collected by filtration under a vacuum, washed with distilled water several times; then transferred to a glass dish and allowed to dry to obtain white powder.

**Preparation of PET@ZnO/DA NCs.** Several samples of the NCs with different amounts of ZnO/DA NPs (1, 3, 5 wt %) were prepared via ultrasonic irradiation through the following procedure: First 0.10 g of the recycled PET (powder) was added into 12 mL of DMAc and sonicated for 15 min. Different amounts of the ZnO/DA filler (1, 3, 5 wt %) subsequently was added to the container (separately). The suspension was sonicated using an ultrasonic liquid processor for 1 h at 50 °C. The solvent was evaporated by placing the resulting mixtures at room temperature until they were dried to obtain PET@ZnO/DA NCs. Scheme 3 shows manufacturing way of PET@ZnO/DA NCs.

### Methodology

The reaction was occurred on a TOPSONICS ultrasonic liquid processor, UP-400 series with a wave of frequency  $20 \pm 1$  kHz and power 100 W (Tehran, I. R. Iran). Fourier transform infrared (FT-IR) spectra of the prepared materials were recorded in the range 4000–400  $\text{cm}^{-1}$  on a Jasco-680 (Japan) Fourier transform spectrometer using the KBr pellet technique. Thermogravimetric (TG) analysis was performed on a STA503 TA instrument by heating rate of  $20 \text{ }^\circ\text{C min}^{-1}$  from ambient temperature to 800 °C in an argon atmosphere. Char yields and the limiting oxygen index (LOI) values were determined using van Krevelen and Hoftzyer numerical method. The X-ray diffraction (XRD) patterns were collected by using a Philips X'Pert MPD X-ray diffractometer. The diffractograms were measured in the range of  $10^\circ$ – $80^\circ$ , using a voltage of 40 kV and Cu K $\alpha$  incident beam ( $k = 1.51418 \text{ \AA}$ ). The microstructure of the samples was investigated by field emission scanning electron microscopy (FE-SEM, Hitachi, S-4160), and transmission electron microscopy (TEM, Philips CM 120, 100 kV). UV/vis measurements of NCs were carried out on a UV/vis/NIR spectrophotometer, JASCO, V-570 in the spectral wavelength range between 200 and 800 nm.

### RESULTS AND DISCUSSION

The ZnO NPs were modified by optically active DA containing L-Alanine amino acid as reported previously.<sup>25</sup> As can be seen from Scheme 2, the existence of the polar groups of DA such as  $\text{NH}_2$  and  $-\text{COOH}$  has been considered as the main factor that can bind to remaining  $-\text{OH}$  groups on the surface of ZnO NPs.<sup>26</sup> Recycled PET, with the different functional groups, was used as a polymeric matrix material for the NCs preparation.  $-\text{COOH}$  groups of DA and the functional groups of PET chains as well as OH groups on the surface of ZnO NPs perform hydrogen bonding. Moreover, the introduction of aromatic moieties along the backbone of the polymer performs  $\pi$ – $\pi$  stacking interactions with modified ZnO/DA NPs (Scheme 3).

#### FT-IR Spectroscopy

Figure 1 shows the acquired FT-IR spectra for the all prepared materials together with the original PET bottle. The presence of O–H on the surface of ZnO NPs is revealed by broad band at  $3500 \text{ cm}^{-1}$  and a broad peak at  $432 \text{ cm}^{-1}$  depict the Zn–O bond stretching [Figure 1(a)].<sup>22,25</sup> There are some characteristic absorption bands related to the imide heterocyclic ring in the spectrum of DA [Figure 1(b)]. Absorption peak at  $1259 \text{ cm}^{-1}$  is resulted from C–O bonds and peaks at  $1779$  and  $1719 \text{ cm}^{-1}$  are assigned to the asymmetrical and symmetrical carbonyl stretching vibrations of the imide ring. The absorption band at  $1348 \text{ cm}^{-1}$  is occasioned from C–N stretching. Also, presence of imide groups is verified by peaks at  $1383$  and  $731 \text{ cm}^{-1}$ .<sup>25,27</sup> The spectrum of modified ZnO with DA [Figure 1(c)] is shown new peaks in compared to the neat ZnO [Figure 1(a)] that can be due to interaction between functional groups of DA and  $-\text{OH}$  groups on the surface of ZnO NPs.

In the present study, the most significant peaks are in different positions from the recycled PET [Figure 1(d)] peaks for bottle spectrum [Figure 1(h)]. For PET there is a peak at  $3541 \text{ cm}^{-1}$  for hydroxyl end groups and  $3430 \text{ cm}^{-1}$  related to C–O overton.<sup>28</sup> There are two peaks at  $3055$  and  $2965 \text{ cm}^{-1}$  due to C–H bond asymmetric stretching (methylene groups). The FT-IR spectrum of PET confirms the presence of a carbonyl group in conjugation with aromatic ring appears at  $1718 \text{ cm}^{-1}$  related to C=O ester carbonyl bond stretching. The second strongest peak at  $1245 \text{ cm}^{-1}$  is due to the asymmetric C–C–O stretching

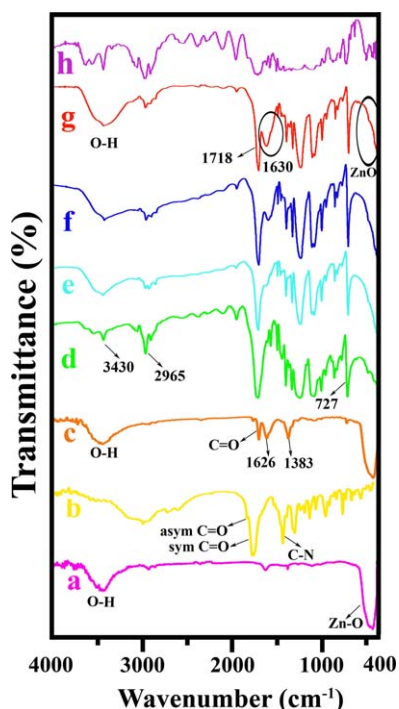


**Figure 1.** FT-IR spectra of (a) neat ZnO NP, (b) DA, (c) ZnO/DA, (d) recycled PET, (e) PET@ZnO/DA NC 1 wt %, (f) PET@ZnO/DA NC 3 wt %, (g) PET@ZnO/DA NC 5 wt %, and (h) PET bottle. [Color figure can be viewed in the online issue, which is available at [wileyonlinelibrary.com](http://wileyonlinelibrary.com).]

involving the carbon in aromatic ring. The aromatic C—H wagging appears at  $727\text{ cm}^{-1}$ .<sup>28–30</sup> The spectrum of PET bottle displays different peaks that can be, because of some additives were omitted in recycling process by the aforementioned dissolution/reprecipitation method. The role of this method is to convert the waste PET into almost pure PET powder and remove any adhesive.<sup>9</sup> The FT-IR spectra of the NCs with 1, 3, 5 wt % of ZnO/DA [Figure 1(e–g)] compared with pure PET exhibited different absorption peaks at 1630 and  $422\text{ cm}^{-1}$  which has been assigned to ZnO NPs and DA capping agent.

#### XRD Patterns

XRD is the most direct technique to identify and quantify material crystallinity. XRD patterns of the recycled PET, pure, and modified ZnO NPs, and PET@ZnO/DA NCs with 1, 3, and 5 wt % of modified ZnO NPs content were conducted and Figure 2 shows the XRD curves. In Figure 2(a), a series of significant peaks of 31.8, 34.4, 36.2, 47.6, 56.6, 62.9, 66.4, 67.9, and 69.1 are observed which are typically associated with reflection from: 100, 002, 101, 102, 110, 103, 200, 112, and 201 crystal planes, respectively, according with hexagonal wurtzite phase of ZnO NPs.<sup>25</sup> The capping agent and ultrasonic irradiation did not influence on the crystalline phase of ZnO NPs and the characteristic peaks were still in accordance with the wurtzite phase of neat ZnO [Figure 2(b)]. The XRD patterns of PET@ZnO/DA NCs indicate that XRD pattern of ZnO NPs has not been changed during the ultrasonication process and using modifier on the NPs surface. Also, according to Figure 2(c), XRD pattern indicates a semicrystalline triclinic structure for recycled PET

polymer.<sup>31</sup> Semicrystalline PET typically shows characteristic crystalline XRD peaks at  $2\theta = 16.1, 17.5, 21.5, 22.7, 24.0, 26.1, 27.8,$  and  $32.5^\circ$ , corresponding to the: 011, 010, 111, 110, 011, 100, 021, 002, 111, and 101 crystal planes, and a broad amorphous halo at  $10^\circ\text{--}35^\circ$ .<sup>32</sup>

In the NCs diffraction patterns [Figure 2(d–f)], intensity of diffraction peaks tends to increase with the increasing of the modified ZnO contents. Also, the degree of crystallinity gradually increased in compare with recycled PET. Increase in crystallinity, can be described with an increase in molecular diffusion that favors the molecular arrangement via ultrasonic irradiation.<sup>31</sup> Through ultrasonication process, released energy from collapse causes a temperature of 500 K and a pressure of 1000 bar that can be the reason for recrystallization.<sup>33</sup> Besides, the solvent treatments have affected the crystallinity of PET due to their solubility within the polymer. The interaction of the solvents with polymer is expected to lead to conceivable recrystallization.<sup>34</sup> It is noticeable that ultrasonication time and power which used in the process was the same for all the prepared NCs and these results depend relatively on the amount of the different NPs content. It seems that NPs enhances crystallization by acting as a heterogeneous nucleation agent.<sup>35</sup> This observation can use in order to hasten the crystallization rate of PET and get the desired morphology and feature.<sup>36</sup>

#### Optical Property Analysis

Figure 3 presents the UV-vis absorption spectra in the region 200–800 nm for recycled PET and PET@ZnO/DA NCs (1, 3, and 5 wt %). ZnO as a semiconductor material can improve photochemical properties of polymers. Absorption increased with more ZnO/DA NPs concentration due to absorbing molecules number. Beer's Law clarified that the concentration of a substance is directly proportional to the absorbance.<sup>37</sup> ZnO as an antibacterial agent, expose to UV light with the wavelength less than 388 nm, can produce radicals ( $\text{O}_2^-$  and  $\text{HO}^\bullet$ ) to destroy

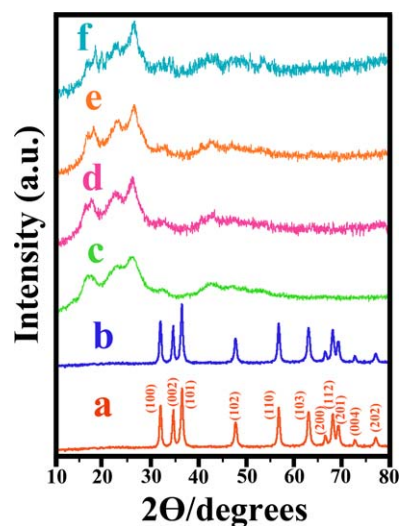


**Figure 2.** The XRD patterns of (a) ZnO NPs, (b) modified ZnO/DA (c) recycled PET, (d) PET@ZnO/DA NC 1 wt %, (e) PET@ZnO/DA NC 3 wt %, (f) and PET@ZnO/DA NC 5 wt %. [Color figure can be viewed in the online issue, which is available at [wileyonlinelibrary.com](http://wileyonlinelibrary.com).]

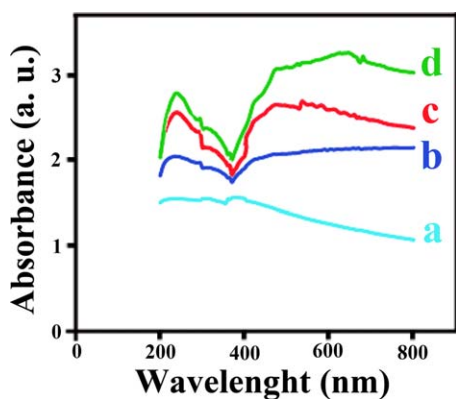


**Figure 3.** Absorption spectra of (a) PET, (b) PET@ZnO/DA NC 1 wt %, (c) PET@ZnO/DA NC 3 wt %, (d) PET@ZnO/DA NC 5 wt %. [Color figure can be viewed in the online issue, which is available at wileyonlinelibrary.com.]

and shrink bacterial cells by reacting with them.<sup>38</sup> Photoactivity of the obtained PET@ZnO/DA NCs has been dramatically changed by combining PET polymer matrix with ZnO/DA. The interfacial interaction between NPs and PET matrix has been ameliorated by the increasing specific surface area of the filler and prevent agglomeration by using organic modifier. Due to the high UV protection nature, ZnO is used as an ideal UV blocker and usually added into cosmetics for ultraviolet protection.<sup>39</sup> In the view of the above mentioned facts, colorless ZnO NPs doping in PET expected to create beneficial NCs especially for the food packaging industry act as a filter.

### Morphological Characterization

In order to observe changes in morphology of the matrix and the prepared NCs and modified NPs, the photographs of the samples were investigated by FE-SEM (Figures 4–6). Shown in Figure 4 are the respective FE-SEM images of ZnO/DA at different magnifications. FE-SEM observation revealed that the shape of modified ZnO NPs is spherical and they are distributed uniformly. For investigation of the morphology, FE-SEM images of the recycled PET samples sonicated in DMAc and ethanol were carried out and compared with those of the recycled PET before ultrasonication at different magnifications [Figure 5(a–f)]. As can be seen in Figure 5(a,b), recycled PET before ultrasonic

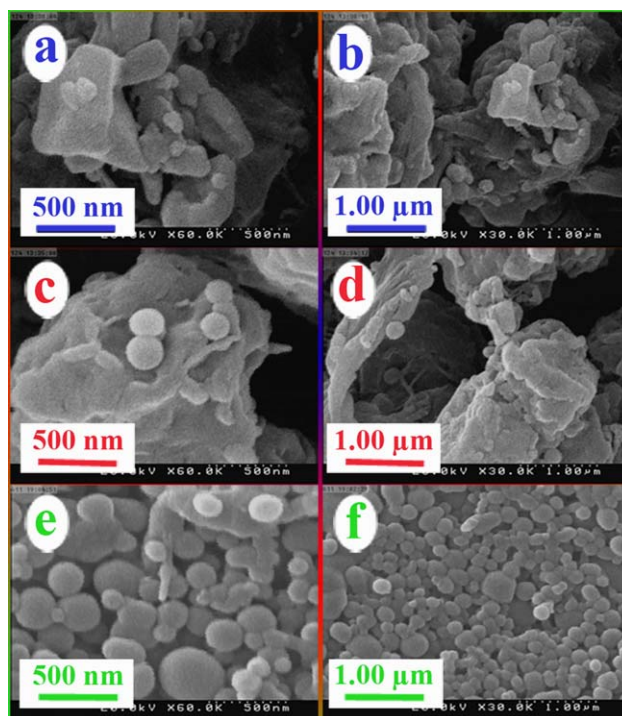


**Figure 5.** FE-SEM images of recycled PET (a,b) before ultrasonic irradiation, (c,d) after ultrasonic irradiation in ethanol, (e,f) after ultrasonic irradiation in DMAc. [Color figure can be viewed in the online issue, which is available at wileyonlinelibrary.com.]

irradiation has irregular morphology and large scatter, which roughly consists of rock-like shapes stacked near each other.

It is interesting to note that safe and easy ultrasonication process with using suitable solvent has changed morphology by reducing PET particle size. The morphological feature of the sonicated PET in ethanol is similar to the un-sonicated sample. It appears particles that sonicated in DMAc compared to the others, have relatively spheroid structured morphology in smaller size. The FE-SEM images of the prepared NCs revealed the nature of particles, in which 1, 3, 5 wt % nano ZnO was added (Figure 6). It can be seen many little particles on PET surface that are relatively homogeneous, without formation of any agglomerates. This indicates that the modifiers functions by aiding the dispersion of the NPs in PET matrix. This aim has

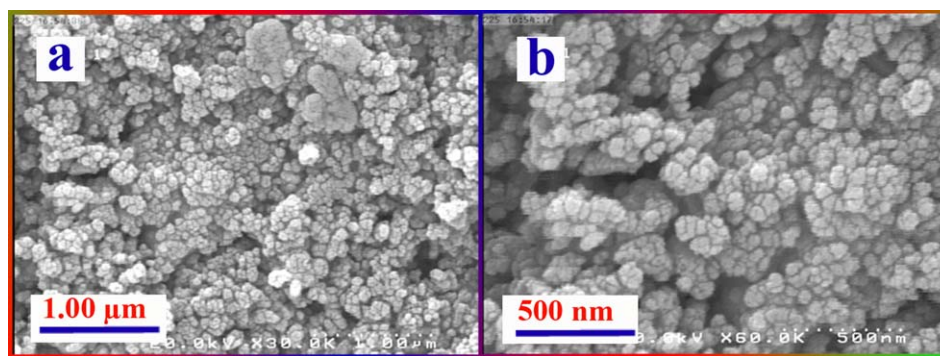


**Figure 4.** FE-SEM images of ZnO/DA at different magnifications. [Color figure can be viewed in the online issue, which is available at wileyonlinelibrary.com.]

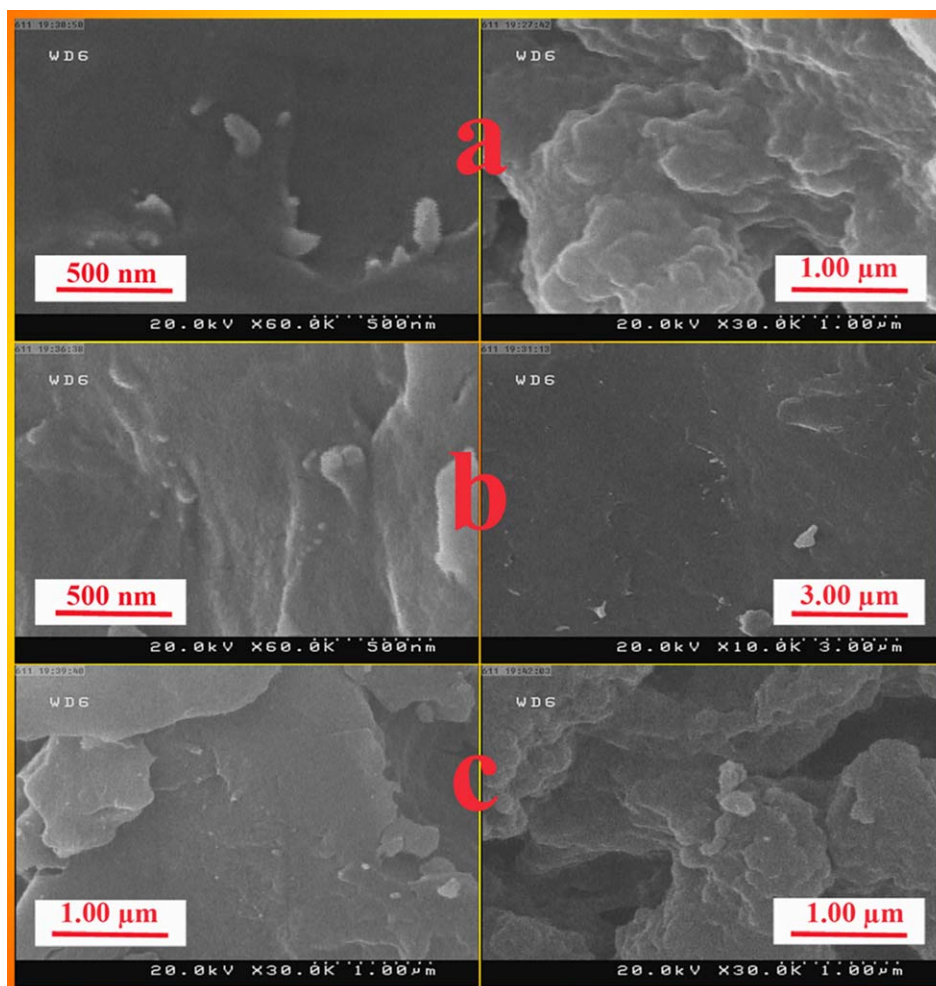


**Figure 6.** FE-SEM images of (a) PET@ZnO/DA NC 1 wt %, (b) PET@ZnO/DA NC 3 wt %, and (c) PET@ZnO/DA NC 5 wt %. [Color figure can be viewed in the online issue, which is available at [wileyonlinelibrary.com](http://wileyonlinelibrary.com).]

attained through strong interfacial bonding exists between the matrix and DA by the different functional groups as mentioned. Also ultrasonication is a useful way to prevent agglomeration.

TEM analysis is a proven and reliable procedure to image native state morphologies of nanoscale soft and hard objects. Figure 7 is the analysis image of the pure [Figure 7(a)] and modified ZnO NPs [Figure 7(b–d)] at different magnifications. A number-frequency histogram is a typical way to present the particle size and its distribution. It can be seen from TEM observations the mean size of about 36 nm, that accumulated from measurements of 26 particles in related histogram. Images show different shape of modified NPs compare to the unmodified NPs.

In Figure 8(a–d), the TEM images of PET@ZnO/DA NC 8 wt % at different magnifications can be seen. TEM observations of the NC confirm that the ZnO particles size is in nanoscale mostly smaller than modified one which can be attributed to effective modifier. Organic coupling agent prevented NPs agglomeration through electrostatic repulsion and steric hindrance between them as well as good interaction with PET matrix.

### Thermogravimetric Analysis

The thermograms of modified ZnO NPs in Figure 9, recycled PET and PET@ZnO/DA NCs in Figure 10 are reported. Also, the corresponding data is shown in Table I. TGA was performed on the prepared NCs to investigate the effect of modified ZnO NPs on thermal stability of the recycled PET matrix. The thermal stability of the polymers was studied on the basis of 10 and 20% weight losses ( $T_{10}$  and  $T_{20}$ , respectively) of the polymers and the residue at 800 °C.

The thermal decomposition temperature of the modified NPs show three distinct weigh loses steps. The first stage to temperature of 150 °C (1 wt %) is due to removal water and moisture attached on the NPs surface and evaporation of solvent used during modification. The second stage that occurs between 150 and 360 °C is mainly related to dehydration process of —OH groups on the surface of NPs. The last step is attributed to the total amount pyrolysis of DA molecules about 360–455 °C.<sup>25</sup>

It is obvious that thermal decomposition for PET@ZnO/DA NCs is similar to pure PET. One step mass-loss of recycled PET undergoes stretching between 370 and 480 °C and losing about 85% of its initial mass. Small mass-loss are observed in the beginning of the thermal

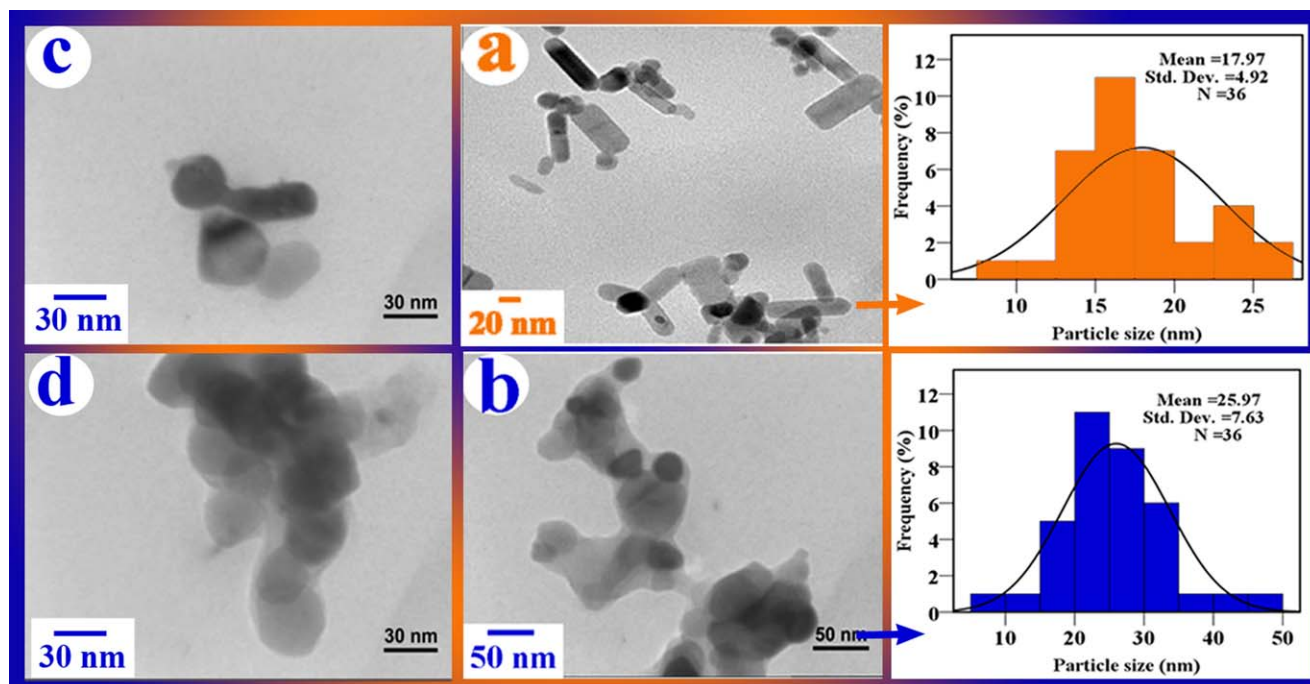


**Figure 7.** TEM images of (a) neat ZnO, (b–d) modified ZnO/DA at different magnifications and related histograms. [Color figure can be viewed in the online issue, which is available at [wileyonlinelibrary.com](http://wileyonlinelibrary.com).]

degradation of PET@ZnO/DA NCs between 250 and 370 °C, which can be evident as a removal of the absorbed small molecules and dehydration process of —OH groups on the NPs surfaces. The weight residue shows that higher amount of char yield is obtained with more NPs content compared with recycled PET.

LOI is a test for characterizing the flammability tendency of polymer that herein is used for test of PET@ZnO/DA NCs and is

defined as the % based on van Krevelen and Hoftyzer equation. Due to linear relationship between LOI and char yield, macromolecules with LOI above 21% are categorized as self-extinguishing materials (oxygen concentration in ambient air is 21%).<sup>25</sup>

$$\text{LOI} = 17.5 + 0.4 \text{ CR} \text{ where CR} = \text{char yield.}$$

For all NCs, LOI results affirm that the LOI increase with further contents of ZnO/DA. For comparing burning behavior and flame retardancy, the pellets of recycled PET and PET@ZnO/DA NC 3 wt % have been prepared and burned on the flame. As can be seen from the Figure 11, burning behavior of the recycled PET [Figure 11(a–d)] is different from the prepared PET@ZnO/DA NC 3 wt % (Figure e–h). Recycled PET without filler, has burned fast after ignition. Due to the resistance of the NC to the burning in the middle of the plate the flame will go around it [Figure 11(f)]. Modified ZnO NPs in matrix has been

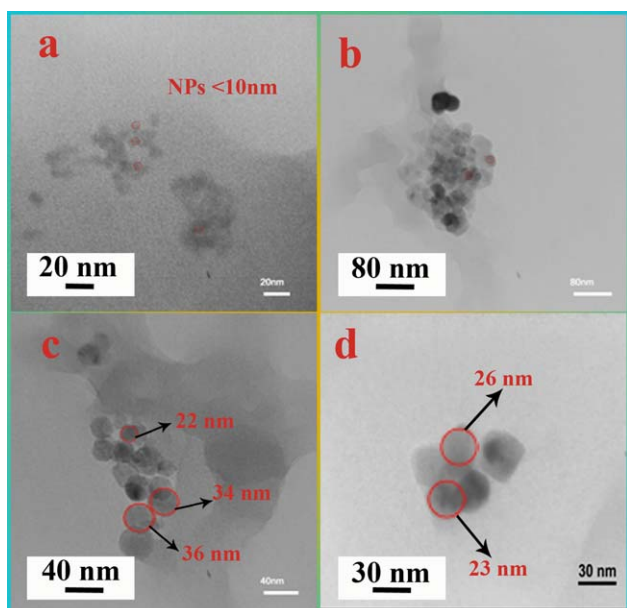


**Figure 8.** TEM images of PET@ZnO/DA NC 3 wt % at different magnifications. [Color figure can be viewed in the online issue, which is available at [wileyonlinelibrary.com](http://wileyonlinelibrary.com).]

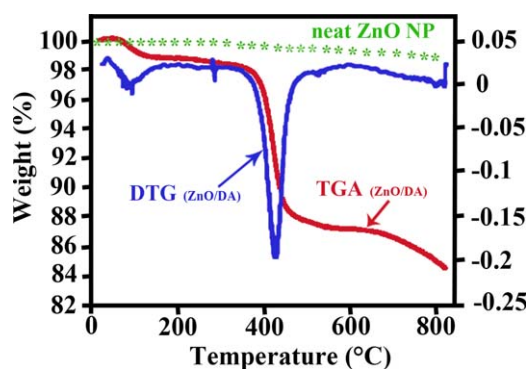


**Figure 9.** TGA thermograms of the neat ZnO, modified ZnO/DA. [Color figure can be viewed in the online issue, which is available at [wileyonlinelibrary.com](http://wileyonlinelibrary.com).]

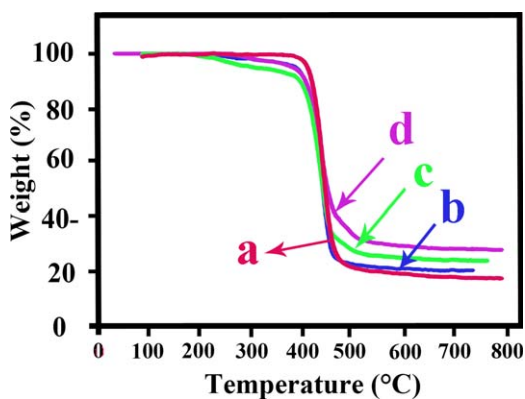


**Figure 10.** TGA curves of (a) PET, (b) PET@ZnO/DA NC 1 wt %, (c) PET@ZnO/DA NC 3 wt %, (d) PET@ZnO/DA NC 5 wt %. [Color figure can be viewed in the online issue, which is available at [wileyonlinelibrary.com](http://wileyonlinelibrary.com).]

resulted in delayed ignition, retarded rate of burning, and reduced smoke emission. These consequences can be due to small size, larger specific area, and strong interfacial interaction between the organic polymer and inorganic NPs because of the many hydroxyls on its surface.<sup>40</sup> It seems that ZnO NPs pro-

mote synergistic effects<sup>41</sup> then can protect the inner matrix and the NCs shape has been kept at the end.

Also, according to Johnson, the  $\Delta H_{\text{comb}}$  values of compounds can determine from LOI:

$$\text{LOI} = 8000 / \Delta H_{\text{comb}}$$

$\Delta H_{\text{comb}}$  is the enthalpy (heat) of a compound combustion with oxygen under standard conditions in J/g.<sup>42</sup>

## CONCLUSIONS

PET bottles waste was recycled by the dissolution/precipitation method. In order to improve the stability and dispersity of ZnO NPs and also, increase the compatibility between ZnO NPs and organic PET matrix, the surface of ZnO NPs was modified by synthesized DA containing L-alanine amino acid. Optically active DA was used as biocompatible, biodegradable, and biosafe organic molecule that has different functional groups. Different amounts of ZnO/DA NPs (1, 3, 5, wt %) were reinforced into the recycled PET matrix and properties of the obtained PET@ZnO/DA NCs were investigated using FT-IR spectroscopy, UV-vis analysis, TGA, and XRD. The morphology of the ZnO/DA NPs and PET@ZnO/DA NCs was examined using FE-SEM and TEM and

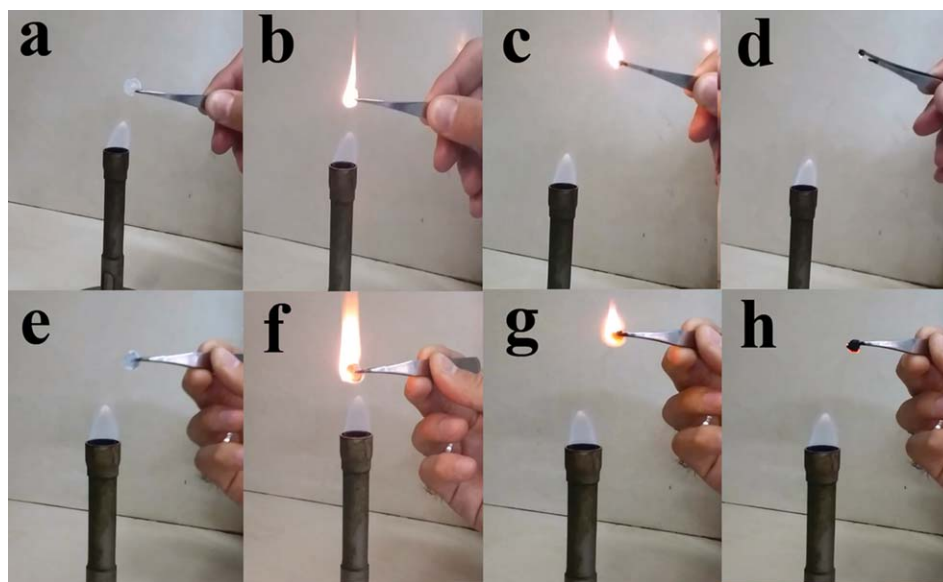


**Figure 11.** Burning behavior of recycled PET (a–d) and PET@ZnO/DA NC 3 wt % (e–h). [Color figure can be viewed in the online issue, which is available at [wileyonlinelibrary.com](http://wileyonlinelibrary.com).]

**Table I.** Thermal Properties of Recycled PET and PET@ZnO/DA NCs

Samples set	Initial weight (mg)	$T_{10}$ (°C) <sup>b</sup>	$T_{20}$ (°C) <sup>a</sup>	Char yield (%) <sup>c</sup>	LOI (%) <sup>d</sup>	$\Delta H_{\text{comb}}$ (kJ/g)
Recycled PET	7.31	420	429	18.0	24.7	35.2
(PET@ZnO/DA) <sub>1</sub> wt %	7.74	404	418	20.2	25.6	31.2
(PET@ZnO/DA) <sub>3</sub> wt %	7.42	395	416	23.7	27.0	29.6
(PET@ZnO/DA) <sub>5</sub> wt %	6.90	405	422	28.2	28.9	27.7

<sup>a</sup> Temperature at which 10% weight loss was recorded by TGA at heating rate of 20 °C/min under an argon atmosphere.

<sup>b</sup> Temperature at which 20% weight loss was recorded by TGA at heating rate of 20 °C/min under an argon atmosphere.

<sup>c</sup> Weight percentage of material left undecomposed after TGA analysis at a temperature of 800 °C under an argon atmosphere.

<sup>d</sup> Limiting oxygen index (LOI) evaluating char yield at 800 °C.



the results showed uniform dispersity and spherical shape of the modified NPs that could be related to effective interaction between particles. Besides ultrasonic irradiation was a beneficial method for particle size reduction in dispersions due to potential in the deagglomeration. The prepared NCs had greater UV-Vis absorption versus recycled PET. This change could be explained by the photoactivity of well-dispersed ZnO/DA NPs. With increasing filler loading in the matrix, the NCS absorption enhanced in UV and visible ranges. Due to UV-vis diagrams of PET@ZnO/DA NCs, they may be suitable candidate for packaging industry. The obtained data by thermal analysis revealed that these NCs showed high char yield in TGA and good LOI values and could be categorized as self-extinguished materials. At least, we can conclude that the presence of organic coupling agent prevented NPs agglomeration effectively through electrostatic repulsion and steric hindrance between NPs as well as decrease surface energy of them and good interaction with PET matrix. Combining PET polymer with modified ZnO/DA NPs can generate materials which are anticipated to have antibacterial activity, biodegradability and biocompatibility properties.

#### ACKNOWLEDGMENTS

The authors wish to express their gratitude to the Research Affairs Division Isfahan University of Technology (IUT), Isfahan, for partial financial support. Further financial support from National Elite Foundation (NEF), Iran Nanotechnology Initiative Council (INIC) and Center of Excellency in Sensors and Green Chemistry Research (IUT) is gratefully acknowledged.

#### REFERENCES

1. Mancini, S. D.; Zanin, M. *J. Appl. Polym. Sci.* **2000**, *76*, 266.
2. Vakili, M.; Fard, M. H. *World Appl. Sci. J.* **2010**, *8*, 839.
3. Tokiwa, Y.; Calabia, B. P.; Ugwu, C. U.; Aiba, S. *Int. J. Mol. Sci.* **2009**, *10*, 3722.
4. Awaja, F.; Pavel, D. *Eur. Polym. J.* **2005**, *41*, 1453.
5. Zhuo, C.; Levendis, Y. A. *J. Appl. Polym. Sci.* **2014**, *131*, 39931. DOI: 10.1002/APP.39931.
6. Siddique, R.; Khatib, J.; Kaur, I. *Waste Manage.* **2008**, *28*, 1835.
7. Lee, J. H.; Lim, K. S.; Hahm, W. G.; Kim, S. H. *J. Appl. Polym. Sci.* **2013**, *128*, 1250.
8. Goje, A. *Polym.-Plast. Technol. Eng.* **2005**, *44*, 1631.
9. Poulakis, J.; Papaspyrides, C. *J. Appl. Polym. Sci.* **2001**, *81*, 91.
10. Hopewell, J.; Dvorak, R.; Kosior, E. *Philos. Trans. R. Soc. B* **2009**, *36*, 2115.
11. Grady, C.; Younos, T. *Int. Water. Technol. J.* **2012**, *2*, 185.
12. Thostenson, E. T.; Chunyu, L.; Tsu-Wei, C. *Compos. Sci. Technol.* **2005**, *65*, 491.
13. Mallakpour, S.; Dinari, M. *Colloids Polym. Sci.* **2013**, *291*, 2487.
14. Rafiei, S.; Riaz, G. H.; Afrasiabi, A. *J. Iran. Chem. Soc.* **2015**, *12*, 87.
15. Xie, Y.; He, Y.; Irwin, P. L.; Jin, T.; Shi, X. *Appl. Environ. Microbiol.* **2011**, *77*, 2325.
16. Wilke, P.; Coger, V.; Nachev, M. *Polymer* **2015**, *61*, 163.
17. Mallakpour, S.; Behranvand, V. *Coll. Polym. Sci.* **2014**, *29*, 2275.
18. Miller, C. E.; Eichinger, B. *Appl. Spectrosc.* **1990**, *44*, 496.
19. Bagabas, A.; Alshammari, A.; Aboud, M. F.; Kosslick, H. *Nanoscale Res. Lett.* **2013**, *8*, 1.
20. Mallakpour, S.; Khani, M. *J. Chil. Chem. Soc.* **2013**, *58*, 1603.
21. Li, S. C.; Li, Y. N. *J. Appl. Polym. Sci.* **2010**, *116*, 29659.
22. Mallakpour, S.; Javadpour, M. *Colloids Polym. Sci.* **2015**, *293*, 2565.
23. Gao, W.; Zhou, B.; Liu, Y. *Polym. Int.* **2013**, *62*, 432.
24. Mallakpour, S.; Ayatollahi, H.; Sabzalian, M. *Polym. Sci. Ser. B* **2014**, *56*, 464.
25. Mallakpour, S.; Behranvand, V. *Des. Monomers Polym.* **2015**, *18*, 79.
26. Mallakpour, S.; Abdolmaleki, A.; Rostami, M. *Polym.-Plast. Technol. Eng.* **2014**, *53*, 1615.
27. Rama Devi, V.; Radha, V.; VijayaKumar, B.; Ravikumar, K.; Vitha, M. *Synth. React. Inorg. Metal-Org. Nano-Met. Chem.* **2010**, *40*, 883.
28. Mamoor, G.; Shahid, W.; Mushtaq, A.; Amjad, U.; Mehmood, U. *Chem. Eng. Res. Bull.* **2013**, *16*, 25.
29. Donelli, I.; Taddei, P.; Smet, P. F.; Poelman, D.; Nierstrasz, V. A.; Freddi, G. *Biotechnol. Bioeng.* **2009**, *103*, 845.
30. Ptiček Siročić, A.; Fijačko, A.; Hrnjak-Murgić, Z. *Chem. Biochem. Eng. Q* **2013**, *27*, 65.
31. Baldenegro-Perez, L. A.; Navarro-Rodriguez, D.; Medellin-Rodriguez, F. J.; Hsiao, B.; Avila-Orta, C. A.; Sics, I. *Polymers* **2014**, *6*, 583.
32. Strain, I.; Wu, Q.; Pourrahimi, A. M.; Hedenqvist, M. S.; Olsson, R. T.; Andersson, R. L. *J. Mater. Chem. A* **2015**, *3*, 1632.
33. Mallakpour, S.; Madani, M. *Polym.-Plast. Technol. Eng.* **2014**, *53*, 423.
34. Oyeleke, G.; Popoola, A.; Adetuyi, A. *J. Polym. Biopolym. Phys. Chem.* **2015**, *3*, 6.
35. Phang, I. Y.; Pramoda, K.; Liu, T.; He, C. *Polym. Int.* **2004**, *53*, 1282.
36. Jiang, X.; Luo, S.; Sun, K.; Chen, X. *Expr. Polym. Lett.* **2007**, *1*, 245.
37. Abdul Nabi, M.; Yusop, R. M.; Yousif, E.; Abdullah, B. M.; Salimon, J.; Salih, N.; Zubairi, S. I. *J. Polym. Sci.* **2014**, *2014*, ID 697809.
38. Lin, H.; Ding, L.; Deng, W.; Wang, X.; Long, J.; Lin, Q. *Adv. Chem. Eng. Sci.* **2013**, *3*, 236.
39. Coltro, L.; Padula, M.; Saron, E. S.; Borghetti, J.; Buratin, A. E. P. *Packag. Technol. Sci.* **2003**, *16*, 15.
40. Laoutid, F.; Bonnaud, L.; Alexandre, M.; Lopez-Cuesta, J. M.; Dubois, P. *Mater. Sci. Eng.* **2009**, *63*, 100.
41. Jiao, C.; Zhuo, J.; Chen, X. *Plast. Rubber. Compos.* **2013**, *42*, 374.
42. Mallakpour, S.; Zadehnazari, A. *JCHE* **2013**, *125*, 203.